Separation Science and Technology
Publication details, including instructions for authors and subscription information:
http://www.informaworld.com/smpp/title~content=t713708471

Modeling of Falling Film Molecular Distillator

Zhang Xubin[a]; Xu Chunjian[a]; Zhou Ming[a]
[a] School of Chemical Engineering and Technology, Tianjin University, Tianjin, China

To cite this Article Xubin, Zhang , Chunjian, Xu and Ming, Zhou(2005) 'Modeling of Falling Film Molecular Distillator', Separation Science and Technology, 40: 6, 1371 — 1386
To link to this Article: DOI: 10.1081/SS-200053027
URL: http://dx.doi.org/10.1081/SS-200053027

Separation Science and Technology, 40: 1371–1386, 2005

ISSN 0149-6395 print/1520-5754 online
DOI: 10.1081/SS-200053027

Modeling of Falling Film Molecular Distillator

Zhang Xubin, Xu Chunjian, and Zhou Ming
School of Chemical Engineering and Technology, Tianjin University, Tianjin, China

Abstract: On the basis of the kinetic equation, a mathematic model for two-components in the presence of an inert gas was developed to describe the falling film molecular distillation process. The heat and mass transfer in liquid film on the evaporating surface and the mass transfer in the vapor phase in the distillation gap are taken into account. This model may show the profiles of temperature and concentration of film and the profiles of density, temperature, and velocity of vapor in consideration of the feed rate, evaporation temperature, and inert gas pressure. The model can be applicable to simulating various operational situations in a falling film molecular distillator. The comparison of the experiment results with the model study results shows a satisfactory qualitative agreement between the experiment and the theory.

Keywords: Falling film still, numerical simulation, molecular distillation, BGK equation

INTRODUCTION

Molecular distillation is generally acknowledged to be the safest method to separate and purify thermally unstable compounds and substances having low volatility. This method is characterized by a short exposure of the distilled liquid to elevated temperatures, high vacuum in the distillation space, and a small distance between the evaporator and condenser. During the molecular distillation process, distillation of heat-sensitive materials is

Received 8 February 2004, Accepted 9 January 2005
Address correspondence to Z. Xubin, School of Chemical Engineering and Technology, Tianjin University, Tianjin 300072, China. E-mail: tjzxb@eyou.com

accompanied by only negligible thermal decomposition and proceeds at rates that can be technologically utilized.

In a falling film molecular distillator, the liquid is introduced in the form of a thin film. As a result of the intensive evaporation from the film surface without boiling, considerable concentration and temperature gradients are formed within the film. Thus, the content of the more volatile component in the film surface is decreased and the film surface is cooler compared to the average film temperature. The nonequilibrium surface evaporation with high mass transfer rates is adversely affected by other factors which lower the separation power and evaporation rate of the process, namely the heat and mass transfer in a liquid film on the evaporating cylinder. In the vapor phase in the distillation gap, the influence of the presence of inert gas, width of distillation gap, orientation of the particle movement, and other factors have to be considered. On the condenser, re-evaporation from the condenser lowers the distillation rate. The rate of this re-evaporation is higher for the more volatile component. All these mentioned effects lower the separation power and the evaporation rate.

A comprehensive model of falling film distillation has not been proposed as yet. Only model studies of partial stages of the process have been presented. Many researchers studied the evaporation under the conditions in which the effect of vapor on the process is neglected. A few scholars investigated the effect of vapor on the process (1–4). Ferron (5) studied the passage of molecules through distillation space by using a four-moment method that cannot investigate the effect of inert gas on the process. Bhandarkar (6), Lutišan (7, 8), and Batistella (9) examined the molecular behavior in distillation space of two-component by the direct Monte Carlo simulation method. But it takes a large amount of computation time and storage.

The present paper offers a mathematical molecular distillation model that describes the process of the heat and mass transfer in the film of the evaporating liquid on the evaporating cylinder, in the gas phase in the distillation gap. The effect of operating and construction parameters on the separation factor and the distillation rate was investigated. The study is expected to provide information on the choice of adequate operation conditions.

MATHEMATICAL DESCRIPTION OF THE PROBLEM

An apparatus for falling-film molecular distillation is shown in Fig. 1. The main part of the installation consists of a cylindrical evaporator surrounded by a condenser jacket. The liquid to be distilled is transported to the evaporating surface. There, it flows down in the form of film and is partly vaporized. The evaporating cylinder is heated internally by the heating fluid with constant temperature, T_w. The condensing cylinder is cooled by the fluid with constant temperature, T_c. In this study, the following assumptions are made: 1) Liquid

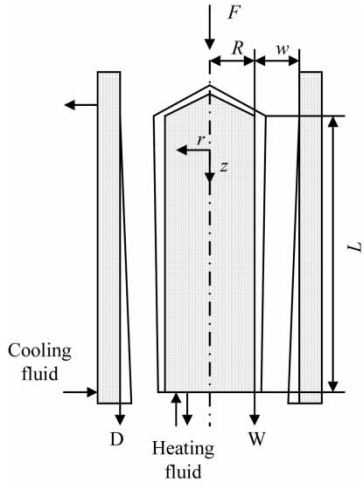

Figure 1. Scheme of the falling-film molecular evaporator.

flow in the steady state, 2) Liquid is Newtonian fluid, 3) Liquid is in laminar flow, 4) No shear forces are exerted on the liquid by the vapor, and 5) Surface tension forces in the axial direction are negligibly smaller than the gravity force. Under such conditions, the velocity profile in the film is given by the equation:

$$u_z = \frac{\rho g}{\mu}\left(\delta(r-R) - \frac{(r-R)^2}{2}\right) \tag{1}$$

The mass flow rate and the continuity equation for the evaporating film give the film thickness:

$$\delta = \left(\frac{3\mu F}{2\pi R\rho^2 g} - \frac{3\mu}{\rho^2 g}\int_0^c \phi_M \, \mathrm{dz}\right)^{1/3} \tag{2}$$

The thermal balance equation can be expressed in the form:

$$u_z \frac{\partial T}{\partial Z} = \frac{k}{\rho c_P}\left(\frac{1}{r}\frac{\partial}{\partial r}\left(r\frac{\partial T}{\partial r}\right)\right) \tag{3}$$

Thermal conductivity, k, and thermal capacity, c_P, are regarded as constants.

The equation of diffusion has the following form:

$$u_z \frac{\partial a_A}{\partial z} = D_{AB}\left(\frac{1}{r}\frac{\partial}{\partial r}\left(r\frac{\partial a_A}{\partial r}\right)\right) \tag{4}$$

Diffusion coefficient, D_{AB}, is to be held constant.

The boundary conditions are:

$$z = 0,\ R \le r \le R + \delta, \quad \begin{cases} a_A = a_{A0} \\ T = T_0 \end{cases}$$

$$r = R,\ 0 \le z \le L, \quad \begin{cases} u_z = 0 \\ \dfrac{\partial a_A}{\partial r} = 0 \\ T = T_w, \quad \text{(constant wall temperature)} \end{cases}$$

$$r = R + \delta,\ 0 \le z \le L, \quad \begin{cases} \dfrac{\partial u_z}{\partial r} = 0 \\ -D_{AB}\rho \dfrac{\partial a_A}{\partial r} = \phi_{A,M} - a_A(\phi_{A,M} + \phi_{B,M}) \\ -k\dfrac{\partial T}{\partial r} = r_v \phi_M \end{cases}$$

Influence of Vapor Phase Resistance

In a real situation, involving vapor transfer through the distillation space, intermolecular collisions occur. This results in the return of part of the vapor molecules back to the evaporating surface. This has an effect on the evaporation efficiency and separation factor. In general, moreover, there is a substantial, net flow of vapor molecules from evaporator to condenser. In order to investigate the behavior of vapor, the following assumptions are made.

1. The behavior of vapor molecules can be described by the nonlinearized Bhatnagar-Gross-Krook (BGK) equation.
2. The molecules leaving each condensed phase are distributed according to the corresponding part of the Maxwellian distribution describing the stationary saturated state at the temperature of the condensed phase.
3. No gradients in velocity caused by external forces are considered.
4. The number of inert gas molecules in the vapor space is constant.

The cylindrical system is shown in Fig. 2, under the previous assumptions, the BGK equation for the steady flows may be (10–13)

$$\zeta_{i,z}\frac{\partial f_i}{\partial z} + \xi_i \cos\varphi \frac{\partial f_i}{\partial r} - \frac{\xi_i \sin\varphi}{r}\frac{\partial f_i}{\partial \varphi} = \frac{1}{\tau_i}(f_{i,e} - f_i) \tag{5}$$

$$f_{i,e} = \frac{n_i}{(2\pi W_i T)^{3/2}} \exp\left(-\frac{(\xi_i \cos\varphi - u)^2 + (\xi_i \sin\varphi)^2 + (\xi_{i,z} - v)^2}{2W_i T}\right) \tag{6}$$

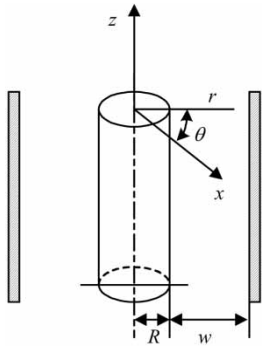

Figure 2. Schematic diagram of coordinate system.

$$n_i = 2\int_{-\infty}^{+\infty}\int_0^{\pi}\int_0^{+\infty} f_i\xi_i \,\mathrm{d}\xi_i \,\mathrm{d}\varphi \,\mathrm{d}\xi_{i,z} \tag{7}$$

$$u_i = \frac{2}{n_i}\int_{-\infty}^{+\infty}\int_0^{\pi}\int_0^{+\infty} \xi_i^2 \cos\varphi f_i\xi_i \,\mathrm{d}\xi_i \,\mathrm{d}\varphi \,\mathrm{d}\xi_{i,z} \tag{8}$$

$$v_i = \frac{2}{n_i}\int_{-\infty}^{+\infty}\int_0^{\pi}\int_0^{+\infty} \xi_{i,z}\xi_i f_i\xi_i \,\mathrm{d}\xi_i \,\mathrm{d}\varphi \,\mathrm{d}\xi_{i,z} \tag{9}$$

$$u = \frac{\sum_i u_i n_i m_i}{\sum_i n_i m_i} \tag{10}$$

$$v = \frac{\sum_i v_i n_i m_i}{\sum_i n_i m_i} \tag{11}$$

$$3nk_bT = \sum_i m_i\left(2\int_{-\infty}^{+\infty}\int_0^{\pi}\int_0^{+\infty}(\xi_i^2 + \xi_{i,z}^2)\xi_i f_i\xi_i \,\mathrm{d}\xi_i \,\mathrm{d}\varphi \,\mathrm{d}\xi_{i,z} - n_i u^2 - n_i v^2\right) \tag{12}$$

Where, $W_i = k_b/m_i$.

The boundary conditions are:

$r = R$, $0 \le z \le L$

$$f_i = \frac{n_{i,\mathrm{h}}}{(2\pi W_i T_\mathrm{h})^{3/2}}\exp\left(-\frac{\xi_i^2 + \xi_{i,z}^2}{2W_i T_\mathrm{h}}\right) \quad 0 \le \varphi < \frac{\pi}{2} \tag{13}$$

$\mathrm{r} = \mathrm{R} + \mathrm{w}$, $0 \le \mathrm{z} \le \mathrm{L}$

$$f_i = \frac{n_{i,\mathrm{c}}}{(2\pi W_i T_\mathrm{c})^{3/2}}\exp\left(-\frac{\xi_i^2 + \xi_{i,z}^2}{2W_i T_\mathrm{c}}\right) \quad \frac{\pi}{2} < \varphi \le \pi \tag{14}$$

Where, for the evaporating molecule

$$n_{i,\mathrm{h}} = p^s_{i,h} X_{i,\mathrm{h}} (k_b T_\mathrm{h})^{-1}$$
$$n_{i,\mathrm{c}} = p^s_{i,c} X_{i,\mathrm{c}} (k_b T_\mathrm{c})^{-1}$$

And, for the inert molecule

$$n_{i,\mathrm{h}} = -(2\pi/W_i T_\mathrm{h})^{1/2} \int_{-\infty}^{+\infty} \int_{\pi/2}^{\pi} \int_0^{+\infty} \xi_i^2 \cos\varphi f_i \, \mathrm{d}\xi_i \, \mathrm{d}\varphi \, \mathrm{d}\xi_{i,z}$$

$$n_{i,\mathrm{c}} = (2\pi/W_i T_\mathrm{c})^{1/2} \int_{-\infty}^{+\infty} \int_0^{\pi/2} \int_0^{+\infty} \xi_i^2 \cos\varphi f_i \, \mathrm{d}\xi_i \, \mathrm{d}\varphi \, \mathrm{d}\, \xi_{i,z}$$

$z = 0,\ R < r < R + w$

$$f_i = \frac{n_{i,\mathrm{u}}}{(2\pi W_i T_\mathrm{u})^{3/2}} \exp\left(-\frac{\xi_i^2 + \xi_{i,z}^2}{2 W_i T_\mathrm{u}}\right) \quad \xi_z > 0 \tag{15}$$

$z = L,\ R < r < R + w$

$$f_i = \frac{n_{i,\mathrm{d}}}{(2\pi W_i T_\mathrm{d})^{3/2}} \exp\left(-\frac{\xi_i^2 + \xi_{i,z}^2}{2 W_i T_\mathrm{d}}\right) \quad \xi_z < 0 \tag{16}$$

Where:

$$n_{i,\mathrm{u}} = -(2\pi/W_i T_\mathrm{u})^{1/2} \int_{-\infty}^{0} \int_0^{\pi} \int_0^{+\infty} \xi_{i,z} \xi_i \cos\varphi f_i \, \mathrm{d}\xi_i \, \mathrm{d}\varphi \, \mathrm{d}\xi_{i,z}$$

$$n_{i,\mathrm{d}} = (2\pi/W_i T_\mathrm{d})^{1/2} \int_0^{+\infty} \int_0^{\pi} \int_0^{+\infty} \xi_{i,z} \xi_i \cos\varphi f_i \, \mathrm{d}\xi_i \, \mathrm{d}\varphi \, \mathrm{d}\xi_{i,z}$$

The evaporation rate $\phi_{i,M}$ at the film surface is given by the following equation:

$$\phi_{i,M} = 2 m_i \int_{-\infty}^{+\infty} \int_0^{\pi} \int_0^{+\infty} \xi_i^2 \cos\varphi f_i \, \mathrm{d}\xi_i \, \mathrm{d}\varphi \, \mathrm{d}\xi_{i,z} \tag{17}$$

Numerical Solution

Eqs. (3), (4), and (5) are changed in the form of finite differences and solved by the finite differences method and iteration scheme. This method has shown high stability. The film thickness was divided into 50 equal intervals, the evaporator length was divided into 100 equal intervals, and the vapor region was divided into 100 intervals in radial and axial respectively.

Comparison between Theoretical Model and Experimental Results

Results of a molecular distillation model study can be compared with experimental data on a mixture of di-(ethylhexyl)-phthalate (EHP) and di-(ethylhexyl)-sebacate (EHS). Measurements of both distillate and residue weights and compositions are available. They were obtained at various temperatures of the evaporation cylinder.

The measurements were performed on a convex short-path evaporator with a cylinder length of 295 mm and a diameter of 30 mm. The distillation gap width was 25 mm.

For the measurements, an EHP-EHS mixture was used at a 1 : 1 molar ratio with a feed rate of about $950\,g \cdot h^{-1}$, the pressure of noncondensable gases ranges from 0.2 to 0.7 Pa (14, 15). Some physical properties of components used are listed in Table 1 and Table 2.

The diffusion coefficient D_{AB} was calculated according to Refs. (16) and (17).

In Fig. 3, a dependence of the composition of distillate from the condenser on the heating cylinder temperature for both the experimental measurements and the model study is shown. This comparison shows that the result obtained from the model study has a satisfactory qualitative agreement with the result obtained from experimental study. The biggest difference does not exceed 5%. Due to omitting the heat transfer from the heating medium to the heating cylinder surface and the heat transfer from the condensing cylinder to the cooling medium, the temperature of film surface in the model is higher than in the actual conditions, moreover, the temperature of the condensing cylinder surface in the model is lower than it is in the actual conditions. This causes the quantity of distillate according to the model to be higher than in the experiment.

Results of Model Study and Discussion

The results of the simulation considering the system dibutylphthalate and dibutylsebacate ((DBP-DBS) are presented. The material constants were

Table 1. Physical properties of components (3, 4)

	EHP	EHS	N_2
$M\ (kg \cdot mol^{-1})$	0.390	0.426	0.028
$r_v \times 10^{-5}\ (J \cdot kg^{-1})$	2.67	2.59	
$\rho\ (kg \cdot m^{-3})$	983	912	
$k \times 10^7\ (W \cdot m^{-1} \cdot K^{-1})$	$3.58 \times c_P \rho (\rho/M)^{0.33}$	$3.58 \times c_P \rho (\rho/M)^{0.33}$	
$c_p\ (J \cdot mol^{-1} \cdot K^{-1})$	612	742	
$d \times 10^{10}$ (m)	8.58	9.02	3.16

Table 2. Viscosity and vapor pressure of component.

	EHP	EHS
$\log_{10}\mu$ (Pa · s) $= A_1 + A_2T^{-1} + A_3T^{-2} + A_4T^{-3}$		
A_1	-14.35	-7.453
A_2	5.234×10^3	1.214×10^3
A_3	-2.882×10^6	-4.218×10^5
A_4	3.954×10^8	9.06×10^7
$\log P^0$(Pa) $= A_5 - A_6T^{-1}$		
A_5	13.74	14.02
A_6	$-5{,}440$	$-5{,}780$

taken from Ref (18). The evaporator radius was assumed to be $R = 0.1$ m, the evaporator height to be $L = 1$ m, and the width of distillation gap to be $w = 20$ mm. Two evaporator temperatures have been selected, 373 and 393 K, and three inert gas partial pressures, 0.0, 0.1 and 0.5 Pa. The temperature of the condenser was 273 K. The temperature of feed was equal to the evaporator temperature. Two feed flow rates, 100 kg · h^{-1} and 50 kg · h^{-1} with a mole fraction of the more volatile component $X_{DBP} = 0.5$, were considered.

Film Temperature

The surface temperature, T_s, of the film is one of most important parameters determining the evaporation rate, ϕ_M, and, subsequently, the distillate rate, D, and composition of the distillate, Y. In Fig. 4, the temperature, T_s, is shown as a function of the film length for different feed rates, F, evaporator temperatures, T_w, and inert gas pressures P_{N_2}. Due to the poor heat transfer

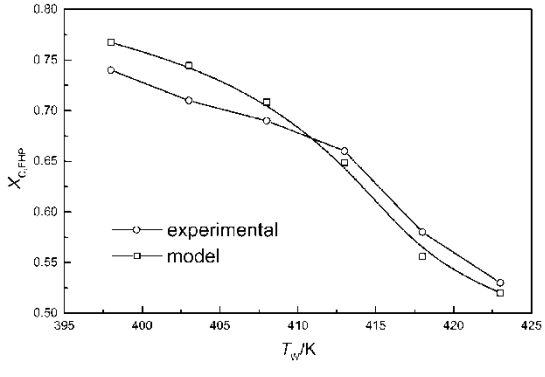

Figure 3. The dependence of the distillate concentration on the heating cylinder temperature for the EHP-EHS mixture.

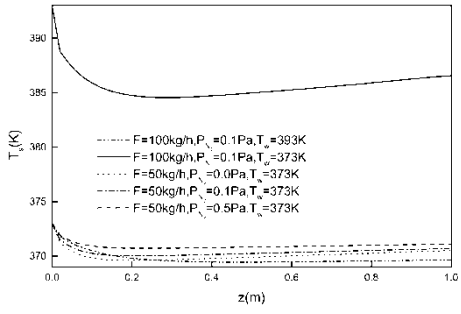

Figure 4. Film surface temperature profiles.

from the bulk of liquid to its surface and the high evaporation rate that develops near the entrance, the temperature decreases quickly. Then, with the increase of distance from the entrance, the evaporation rate decreases, and the temperature, T_s, increases slowly. It can be seen that the temperature changes slightly at large feed rate, low evaporator temperature, and high inert gas pressure. Figure 5 shows temperature profiles in the film for different values of the dimensionless film length. Due to the self-cooling effect of the interface from poor heat transfer from the bulk of the liquid to its surface, where evaporation takes place at the free surface of the liquid, a temperature gradient in the film on the evaporating cylinder is presented.

Concentration Profile

Figure 6 shows the concentration profiles at the surface of the liquid film for different feed rates, F, evaporator temperatures, T_w, and inert gas pressures, P_{N_2}. During distillation, the liquid phase becomes poorer in its more volatile

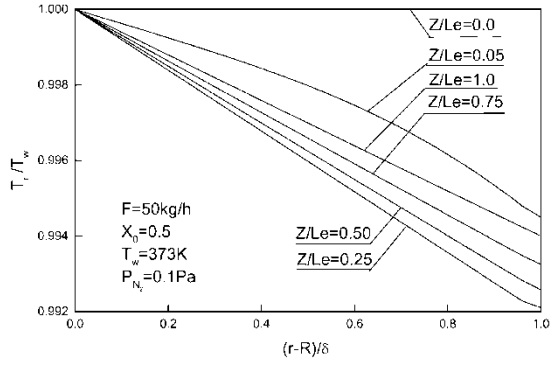

Figure 5. Temperature profiles in the film.

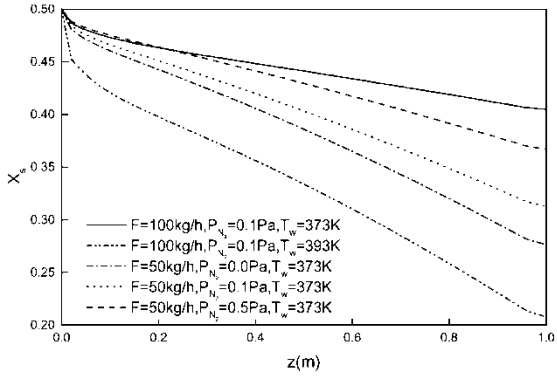

Figure 6. Film surface concentration profiles.

component. Concentration gradient is large for small feed rate, high evaporator temperature, and small inert gas pressure. For instance, for $T_w = 373\,\mathrm{K}$ and $P_{N_2} = 0.1\,\mathrm{Pa}$, the mole fraction of DBP, X_{DBP}, decreases from 0.5 to about 0.405 at a feed rate of $F = 100\,\mathrm{kg \cdot h^{-1}}$, and it decreases from 0.5 to about 0.313 at $F = 50\,\mathrm{kg \cdot h^{-1}}$. For $F = 100\,\mathrm{kg \cdot h^{-1}}$ and $P_{N_2} = 0.1\,\mathrm{Pa}$, X_{DBP} decreases from 0.5 to about 0.405 at $T_w = 373\,\mathrm{K}$, and it decreases from 0.5 to about 0.208 at $T_w = 393\,\mathrm{K}$. For $F = 50\,\mathrm{kg \cdot h^{-1}}$ and $T_w = 373\,\mathrm{K}$, X_{DBP} decreases from 0.5 to about 0.277 at inert gas pressure $P_{N_2} = 0.0\,\mathrm{Pa}$, from 0.5 to about 0.313 at $P_{N_2} = 0.1\,\mathrm{Pa}$, and from 0.5 to about 0.367 at $P_{N_2} = 0.5\,\mathrm{Pa}$. Figure 7 shows concentration profiles in the film for different dimensionless lengths. Due to the low diffusion rate of the more volatile component from the interior of the film to the interface, where the more volatile component is rapidly vaporized, a concentration gradient in the film on the evaporating cylinder is produced.

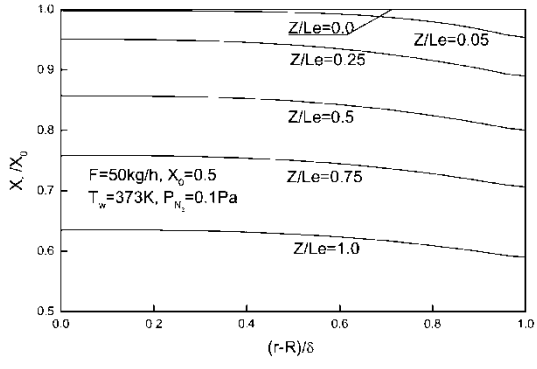

Figure 7. Concentration profiles in the film for different dimensionless lengths.

Evaporation Rate and Distillate Rate

Axial temperature gradients at the liquid surface produce a change in the evaporation rate that itself is temperature dependent. Also the change of surface concentration along the evaporator causes a reduction of the evaporation rate.

Figure 8 presents the evaporation rate of the mixture plotted against the feed rate, the evaporator temperature, and the inert gas pressure. It can be seen from Fig. 8 that the change in evaporation rate is strongly affected by the evaporator temperature and inert gas pressure. The diagrams show that the evaporation rate changes most strongly in the inlet region, on account of the high temperature and concentration gradients at the film surface. The temperature of liquid must be controlled, in order to avoid decomposition of the product. With the increase of evaporator temperature and the decrease of inert gas pressure, the evaporation rate increases. There is higher molecular density in the distillation gap for the concave arrangement, with the consequence that there is greater resistance toward mass transfer across the gap. So, the evaporation rate for the convex arrangement (evaporation from the outer surface of the inner cylinder and condensation at the inner surface of the outer cylinder) is higher than for the concave arrangement (evaporation from the inner surface of the outer cylinder).

The distillate rate is one of the target parameters of distillation. The influence of the different parameters on the total distillate flow rate is presented in Fig. 9. As Fig. 9 shows, for example, for a constant feed rate, $F = 100\,\mathrm{kg \cdot h^{-1}}$, and inert gas pressure, $P_{N_2} = 0.1\,\mathrm{Pa}$, the distillate mass flow rate depends strongly on the evaporator temperature. The following values were obtained for the apparatus under investigation: $D = 57.10\,\mathrm{kg \cdot h^{-1}}$ for $T_w = 393\,\mathrm{K}$ and $D = 20.39\,\mathrm{kg \cdot h^{-1}}$ for $T_w = 373\,\mathrm{K}$. Moreover, the inert gas pressure influences markedly the mass flow rate of

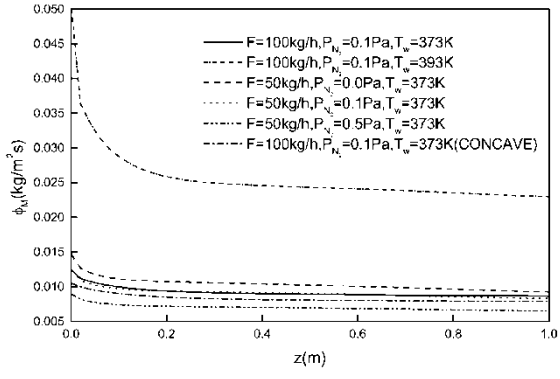

Figure 8. Evaporation rate profiles.

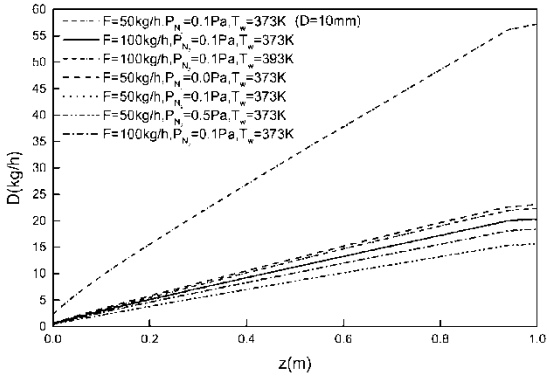

Figure 9. Dependence of distillate flow rate on the evaporating cylinder height.

distillate. For a constant feed rate, $F = 50\,\mathrm{kg \cdot h^{-1}}$, and evaporator temperature, $T_w = 373\,\mathrm{K}$, the following values were obtained: $D = 23.58\,\mathrm{kg \cdot h^{-1}}$ for $P_{N_2} = 0.0\,\mathrm{Pa}$, $D = 20.80\,\mathrm{kg \cdot h^{-1}}$ for $P_{N_2} = 0.1\,\mathrm{Pa}$, and $D = 16.23 = \mathrm{kg \cdot h^{-1}}$ for $P_{N_2} = 0.5\,\mathrm{Pa}$. The distillate rate, D, decreases when the width between the evaporator and condenser increases. However, an increase of the distance between evaporator and condenser causes only a slight decrease of the distillate rate for a lower inert gas pressure.

Separation Factor and Distillation Composition

Both separation factor and the composition of the distillate are functions for the operating parameters studied. Moreover the composition of the distillate is one of the target parameters of the distillation.

Under the conditions of molecular distillation, the separation factor depends strongly on distillation temperature. It decreases with increasing distillation temperature, hence, also the concentration of the more volatile component in the distillate. Separation factor along the evaporator is shown in Fig. 10. The dependence of the distillate concentration on the evaporator height is presented in Fig. 11. The decrease in composition of the more volatile component in the distillate is caused by the change of X_s along the evaporator. It is sharper with an increasing evaporator temperature T_w. Both the concentration of the more volatile factor and separation factor for low feed rate are lower than are ones for high feed rate. This is caused by a decrease in the thickness of the film that, at the same evaporator wall temperature, causes the increase of the film surface temperature. Due to the collisions of molecules, some of the evaporated molecules return to the evaporating surface. For high inert gas pressure, the number of return molecules increases, in other words, the resistance to the mass transfer across the

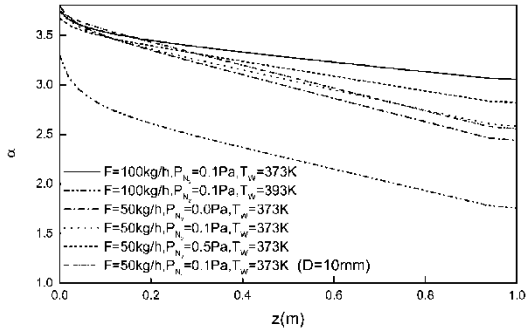

Figure 10. Dependence of separation factor on the evaporating cylinder height.

distillation gap increases. This causes the decrease of the evaporation rate. And it follows from the kinetic equation of gases that the probability of return is greater for lighter molecules (those of the more volatile component). This results in the slight decrease of the temperature and the concentration of the evaporation film surface. Then, the change of the separation factor and the composition of the distillate for high inert gas pressure is smaller. So, the separation factor and the composition of the more volatile component in the distillate at the ends of the condenser are lower for lower inert gas pressure. But the mass flow rate of the distillate is higher for lower inert gas pressure. A dependence of the separation factor and the distillate concentration on the geometry of the distillation space is weak with either the convex and concave arrangement of the distillation space or with the distance between the evaporator and condenser.

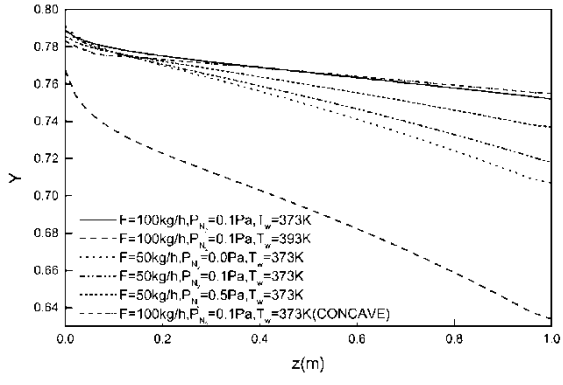

Figure 11. Dependence of distillate concentration on the evaporating cylinder height.

CONCLUSION

The simulation of a falling film molecular distillator has lead to the following important observations concerned with the behavior of the variables in the liquid film and in the vapor phase. There are radial and axial temperature gradients and concentration gradients in the liquid film. The concentration of the more volatile component decreases along the flow path. It is shown that the effect of collisions among the evaporating molecules, and also with the inert gas in the vapor phase, can't be neglected. In real conditions, the evaporation rate is smaller than that given by the equation of Langmuir.

The higher distillate rate can be obtained for the higher feed rate and evaporator temperature. But the increase of the evaporator temperature causes a distinct decrease of the separation factor. The increase of the inert gas pressure brings about a slight increase of the separation factor. In this case too, a marked decrease of distillate rate is observed. Decreasing of the distance between the evaporator and condenser brings about an increase of the distillate rate. These results indicate that the choice of the adequate operation conditions must be made considering the overall effects.

NOMENCLATURE

a	Mass fraction in liquid
d	Molecule diameter, m
D	Distillate rate, $\mathrm{kg \cdot h^{-1}}$
D_{AB}	Diffusion coefficient, $\mathrm{m^2 \cdot s^{-1}}$
F	Feed rate, $\mathrm{kg \cdot h^{-1}}$
f	Velocity distribution function
f_e	Maxwell distribution function
g	Gravitational acceleration, $\mathrm{m \cdot s^{-2}}$
i	Component in a mixture
k	Thermal conductivity, $\mathrm{W \cdot m^{-1} \cdot K^{-1}}$
k_b	Boltzmann constant, $\mathrm{J \cdot K^{-1}}$
L	Height of evaporator, m
m	Mass of a molecule, kg
M	Molar mass, $\mathrm{kg \cdot mol^{-1}}$
n	Molecular number density
P	Pressure, Pa
r_v	Evaporation enthalpy, $\mathrm{J \cdot kg^{-1}}$
r	Radial coordinate
R	Radius of evaporator
T	Temperature, K
u_z	Velocity of film flow, $\mathrm{m \cdot s^{-1}}$
u, v	r, z components of mean flow velocity of gas, $\mathrm{m \cdot s^{-1}}$

w	Distance between evaporation surface and condensation surface, mm
W	Special gas constant, $J \cdot K^{-1} \cdot kg^{-1}$
x, z	Rectangle coordinate system
X	Molecular fraction in liquid

Greek

α	Separation factor
δ	Film thickness, m
μ	Viscosity, $N \cdot s \cdot m^{-2}$
ρ	Density, $kg \cdot m^{-3}$
τ	Collision time, s
ϕ_M	Evaporation rate, $kg \cdot m^{-2} \cdot s^{-1}$
ϕ	Angular coordinate, rad
ξ	Molecule velocity, $m \cdot s^{-1}$

Subscript

A	More volatile component
B	Less volatile component
c	Condensation surface
d	Down battery
e	Equilibrium
f	Film
h	Evaporation surface
i	Component in a mixture
r, ϕ, z	Cylindrical coordinate system
s	Film surface
u	Upper battery
w	Wall

Superscript

s	Saturation

ACKNOWLEDGMENT

Supported by National Natural Science Foundation of China (No.20136010).

REFERENCES

1. Ruckenstein, E. and Hassink, W. (1983) The conbined effect of diffusion and evaporation on the molecular distillation of ideal binary liquid mixture. *Sep. Sci. Technol.*, 18 (6): 523–545.

2. Kawala, Z. and Stephan, K. (1989) Evaporation rate and separation factor of molecular distillation. *Chem. Eng. Technol.*, 12: 406–413.
3. Kawala, Z. (1992) Modeling of short-path high vacuum distillation. *Inst. Chem. Symp. Ser 128. Distillation and Adsorption*, B195–B201.
4. Cvengroš, J., Štefan, P., Miroslav, M., and Juraj, L. (2001) Film wiping in the molecular evaporator. *Chem. Eng. J.*, 81: 9–14.
5. Ferron, J.R. (1986) Evaporation and condensation of mixtures under rarefied conditions. *Ind. Eng. Chem. Fundam.*, 25: 594–602.
6. Bhandarkar, M. and Ferron, J.R. (1991) Simulation of rarefied vapor flows. *Ind. Eng. Chem. Res.*, 30: 998–1007.
7. Lutišan, J. and Cvengroš, J. (1995) Mean free path of molecules on molecular distillation. *Chem. Eng. J.*, 56: 39–50.
8. Lutišan, J. and Cvengroš, J. (1995) Effect of inert gas pressure on the molecular distillation process. *Sep. Sci. Technol.*, 30 (17): 3375–3389.
9. Batistella, C.B., Maciel, M.R.W., and Filho, R.M. (2000) Rigorous modeling and simulation of molecular distillators: development of a simulator under conditions of non ideality of the vapor phase. *Comput. Chem. Eng.*, 24: 1309–1315.
10. Chapman, S. and Cowling, T.G. (1971) *The Mathematical Theory of Non-Uniform Gases*, 2nd Ed.; Cambridge Univ. Press: Cambridge.
11. Yen, S.M. (1984) Numerical solution of the nonlinear Boltzmann equation for non-equilibrium gas flow problem. *Ann. Rev. Fluid. Mech.*, 16: 67–97.
12. Bhatnagar, P.L., Gross, E.P., and Krook, M. (1954) A model for collision processes in gases. *I. Phys. Rev.*, 94: 511–525.
13. Sofonea, V. and Sekerka, R.F. (2001) BGK models for diffusion in isothermal binary fluid systems. *Physica A*, 299: 494–520.
14. Tkáč, A. and Cvengroš, J. (1978) Continuous processes in wiped films. 1. Multistage molecular distillation in an arrangement with a single convex-shape evaporator body. *Ind. Eng. Chem. Process Des. Dev.*, 17 (3): 242–245.
15. Cvengroš, J. and Tkáč, A. (1978) Continuous processes in wiped films. 2. Distilling capacity and separating efficiency of a molecular evaporator with convex evaporating surface. *Ind. Eng. Chem. Process Des. Dev.*, 17 (3): 246–251.
16. Vignes, A. (1966) Diffusion in binary solutions. *Ind. Eng. Chem. Fundam.*, 5 (2): 189–199.
17. Reddy, K.A. and Doraiswamy, L.K. (1967) Estimating liquid diffusivity. *Ind. Eng. Chem. Fundam.*, 6 (1): 77–79.
18. Micov, M. and Lutišan, J. (1997) Balance equations for molecular distillation. *Sep. Sci. Technol.*, 32 (18): 3051–3066.